Available online at www.sciencedirect.com
SCIENCE DIRECT®
ELSEVIER
International Journal of Solids and Structures 43 (2006) 569–582
INTERNATIONAL JOURNAL OF SOLIDS and STRUCTURES
www.elsevier.com/locate/ijsolstr

Incremental deformation and penetration analysis of deformable projectile into semi-infinite target

H. Khoda-rahmi [a], A. Fallahi [b,*], G.H. Liaghat [c]

[a] *Department of Mechanical Engineering, Imam Hossein University, Tehran, Iran*
[b] *Department of Mechanical Engineering, Amirkabir University of Technology, Tehran, Iran*
[c] *Engineering Department, Tarbiat Modarres University, Tehran, Iran*

Received 25 September 2004; received in revised form 15 June 2005
Available online 9 September 2005

Abstract

In this paper, a new analytical method for projectile deformation and penetration into a semi-infinite target has been developed. This method is based on separated, successive and incremental steps. In deformation step, the target assumed rigid and the increment of projectile deformation was evaluated, whilst in penetration step, the projectile assumed rigid and the increment of penetration was evaluated. These sequential steps continued untill the projectile stopped.

Furthermore, a series of ballistic tests have been carried out with ogival projectiles with striking velocity of 600–900 m/s. The projectiles and target plates material has been chosen from 4 types of steel. In this way, 210 tests for 48 combinations of projectile, target and velocity have been carried out. Numerical simulation has been also performed using the LS-DYNA code.

Comparison between the depth of penetration obtained by this analytical method and those of the experimental and numerical ones shows a good agreement.

Keywords: Penetration; Deformable projectile; Semi-infinite target; Numerical simulation; Ballistic test

1. Introduction

Many analytical models have already been presented for penetration analysis of projectiles into target plates, but due to some complications and scientific advances, investigators' efforts have continued to develop new methods to solve the problems. Although some of these efforts are related to the new

* Corresponding author. Tel.: +09821 66405844; fax: +09821 66419736.
E-mail addresses: hkhdrhmi@ihu.ac.ir (H. Khoda-rahmi), afallahi@aut.ac.ir (A. Fallahi).

0020-7683/$ - see front matter © 2005 Elsevier Ltd. All rights reserved.
doi:10.1016/j.ijsolstr.2005.06.072

problems, because of projectile and target developments, studies are still done to solve fundamental and basic problems.

In most previous models, developed for penetration analysis of small calibre and ogival projectile with the striking velocity up to 1000 m/s, projectiles have been assumed rigid. Although the assumption of rigidity for a projectile is in the safe side in armor plate design, considering the projectile deformation during penetration process is an interesting and of course complicated subject for theoretical study and optimum design of armors.

As a review of the important analytical models, we may point out to the works carried out by Recht (1967), by approximating of resistant force on projectile (Forrestal et al., 1988, 1991) based on spherical and cylindrical cavity expansion theories and approximating of resistant force (Dikshit and Sundararajan, 1992; Liaghat and Malekzadeh, 1999) by balancing the rate of dissipated work in target with kinetic energy changes of projectile (Yarin et al., 1995; Roisman et al., 1997; Yossifon et al., 2001) by considering a potential function and calculating the velocity and stress fields in elastic and plastic regions of target, and Chen and Li (2002), by using dynamic cavity expansion theory for ogival, conical and blunt projectiles and metalic, concrete and soil targets, have presented models for penetration analysis of rigid projectiles into semi-infinite metallic targets.

In most analytical models that projectile deformation has been considered, the projectile is assumed to be a long rod with cylindrical geometry and striking velocity more than 1000 m/s. For instance (Alekseevskii, 1966; Tate, 1967) by modifying Bernoulli equation and considering strength parameters of projectile and target (Woodward, 1982) by a one-dimensional model and considering projectile and target as two striking cylinders in mushrooming and erosion cases (Jones and Gillis, 1987) by defining a relation for pressure and considering mushrooming strain (Luk and Piekutowski, 1991) by assuming three phases including head formation, steady and secondary penetration, as well as solving survival and motion equations for every phase (Yaziv and Riegel, 1993) by modifying integral theory (Ravid and Bodner, 1994) by a two-dimensional model based on dynamic plasticity, and balancing the rate of total work on projectile and target (Roisman et al., 2001) by assuming a potential function for velocity and approximating stress fields in projectile and target, and Rubin and Yarin (2002) by developing a algebraic generalized formula for eroding and rigid penetration have considered projectile deformation in penetration process in different ways.

Recently, Chen and Li (2004) found a transition point between the rigid- projectile penetration and the semi-hydrodynamic penetration. Also they have discussed on upper and lower limit of this regimes.

The different regimes of projectile penetration into target can be defined as follows:

(a) Rigid projectile penetration.
(b) Penetration of deformable projectile, without erosion.
(c) The semi-hydrodynamic regime at high velocity with erosion (the range of validation of Tate's model).
(d) The hydrodynamic regime at hypervelocity impact.

The method presented in this paper, related to case (b), which means deformable projectile without erosion. The projectile has been assumed cylindrical with ogival nose and striking velocity up to 1000 m/s. A method has been presented to describe projectile deformation and penetration in successive steps.

For validation, a series of terminal ballistic tests and numerical simulations have been also carried out for comparison. The details are reported in Khodarahmi et al. (2003) works.

2. Description of incremental deformation and penetration method

In this method, two processes of deformation and penetration of the projectile are calculated successively, in small time increments. In each deformation step of solution, the target surface is assumed rigid

and the projectile deforms without penetration, and the increments of projectile deformation and decrease of velocity are calculated. In the next (penetration) step, the projectile is assumed rigid and penetrates into the target, and the increment of penetration of the rigid projectile is calculated (Fig. 1). These sequential steps continue until the projectile stops.

The results of the deformation step, including the decrease of velocity, the length reduction and the geometry changes are considered in the next (penetration) step. Then, in the penetration step, the decrease of projectile velocity due to resistance of the target surface are considered in the next (deformation) step.

The assumptions considered and the reasons are as follows:

(1) After initially transient phase of impact, the contact surface between the projectile and target has been assumed as a part of sphere, then with increasing of deformation and penetration, and after inversion of projectile nose material it will become as hemisphere with cylindrical extension. Based on this assumption, the fundamental differential equations of Hawkyard's model (1969), presented for analysis of cylindrical projectile impacted to a rigid flat surface, with some changes, has been applied for analyzing the impact of ogival projectile to a rigid spherical cavity in projectile deformation steps. Also the differential equations of Forrestal's model (1988, 1991), presented for penetration analysis of rigid projectile with spherical nose, have been used in rigid penetration steps, by making some changes.
(2) Based on experimental results, obtained by Khodarahmi et al. (2003), the diameter of cavity is near twice the projectile diameter in the range of applied velocities. Thus the cavity diameter has been assumed equal to twice the projectile diameter in this model, for simplicity.
(3) In this investigation, the added mass and projectile erosion have not been considered, thus the mass of projectile was assumed constant.
(4) It has been found that the friction coefficient in contact surface is dependent to current velocity of projectile. Also the parametric studies, analytically done by Khodarahmi et al. (2003) have shown that with increasing of the friction coefficient from 0.05 to 0.15, the penetration depth would decrease near to 6%; therefore this coefficient has been assumed constant, equal to 0.1, for simplicity.

A computational program has been developed after modeling the physical phenomena. In this program, deformation and rigid penetration steps are calculated by separated subroutines. The results of each step,

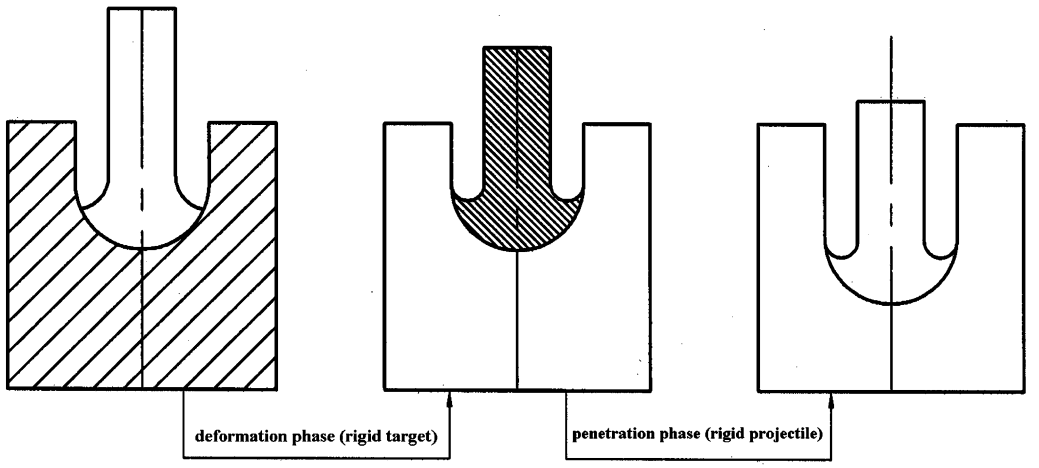

Fig. 1. Sequential deformation and penetration steps.

calculated in a subroutine, are passed to other subroutine as imported data. These successive iterations continue till the velocity of projectile becomes zero. Then, the total depth of penetration and the final length of projectile are obtained.

2.1. Deformation of the projectile impacted to rigid spherical cavity

By assuming spherical surface of cavity in an intermediate deformation step, the striking of a cylindrical projectile to a rigid spherical cavity has been analyzed. Then this analysis, with some changes, was developed for an ogival projectile. After striking a cylindrical projectile to a rigid surface, first an elastic stress wave moves along the projectile and then, a plastic wave propagates with lower velocity as plastic deformation. During each step of deformation an element of the projectile with length $\mathrm{d}x$ and cross-section A_0 passes through the plastic wave front and deforms to a layer with thickness $\mathrm{d}y$ and area A, according to the geometry of cavity with radius r (Fig. 2). Based on kinematics of deformation, the following relations can be written:

$$\mathrm{d}x = \mathrm{d}s + \mathrm{d}y \tag{1}$$

$$\frac{\mathrm{d}s}{\mathrm{d}t} = V \tag{2}$$

where V and $\mathrm{d}s$ are the velocity and the displacement increment of free end of the projectile, respectively.

Using mass conservation we have:

$$A_0\,\mathrm{d}x = A\,\mathrm{d}y \tag{3}$$

Based on energy conservation and balancing of kinetic energy decrease with plastic work during time $\mathrm{d}t$, similar to the Hawkyard's method, we may write:

$$\frac{1}{2}\rho_{\mathrm{p}}V^2 = Y_{\mathrm{p}}[\ln(A/A_0) - (1 - A_0/A)] \tag{4}$$

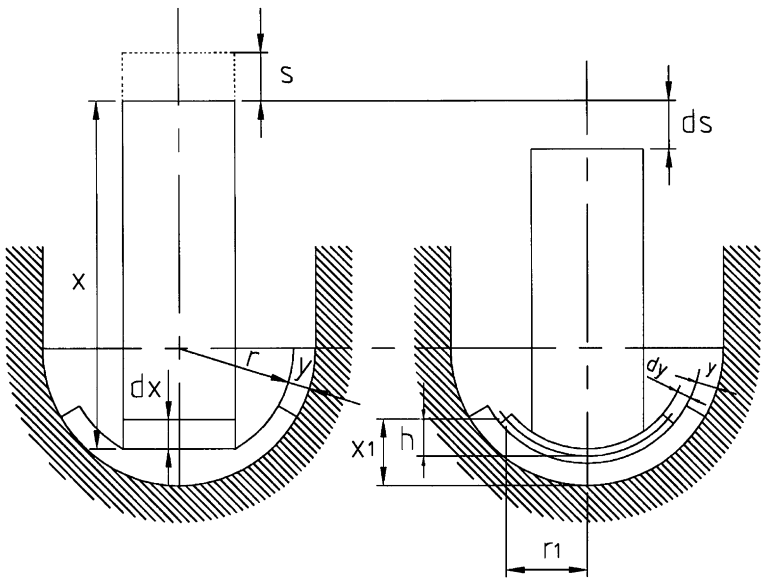

Fig. 2. Deformation modeling of cylindrical projectile impacted to rigid spherical cavity.

where Y_p and ρ_p are yield strength and density of the projectile, respectively. Also, the equation of motion for non-deformed portion of the projectile is

$$Y_p A_0 = -\rho_p x A_0 \frac{dV}{dt} \tag{5}$$

where x is non-deformed length of the projectile.

The radius of cavity at current time is obtained versus initial radius R, and total thickness of previous deformed elements y as (Fig. 2):

$$r = R - y \tag{6}$$

Also the height of edge of the deformed element with respect to natural surface is obtained by using the area of spherical surface A as

$$h = A/2\pi\left(r - \frac{dy}{2}\right) \tag{7}$$

The position of edge of deformed element, with respect to the coordinate system fixed on bottom of cavity is obtained by

$$x_1 = y + \frac{dy}{2} + h \tag{8}$$

$$r_1 = \sqrt{\left(r - \frac{dy}{2}\right)^2 - \left(r - h - \frac{dy}{2}\right)^2} \tag{9}$$

where x_1 and r_1 are positions in axial and radial directions, respectively.

In an independent problem of deformation analysis of a projectile, impacted to a rigid cavity surface, final profile of projectile, including deformed and non-deformed lengths may be obtained by solving Eqs. (1)–(5) and using relations (6)–(9).

In incremental deformation and penetration method in each deformation step, by considering a time increment dt, the increments of displacement of free end (ds), initial thickness of deformed element (dx), thickness of the element after deformation (dy), decrease of projectile velocity (dV) and area A can be obtained. The new values of these variables are calculated from the values in current step m and their increments by following relations:

$$s^{m+1} = s^m + ds \tag{10}$$

$$x^{m+1} = x^m - dx \tag{11}$$

$$y^{m+1} = y^m + dy \tag{12}$$

$$V^{m+1} = V^m - dV \tag{13}$$

Also, the radius of spherical cavity at the end of the step is

$$r^{m+1} = r^m - dy \tag{14}$$

The next step of solution (penetration step) starts after modifying the variables.

In the case of cylindrical projectile with ogival nose (Fig. 3), for each small dx increment of projectile length, the geometry is near to a cylindrical increment. Thus above relations may be used after correction of the cross-section. The initial cross-section of each element is a function of x-position and obtained by

$$A_x = \pi r_x^2 \tag{15}$$

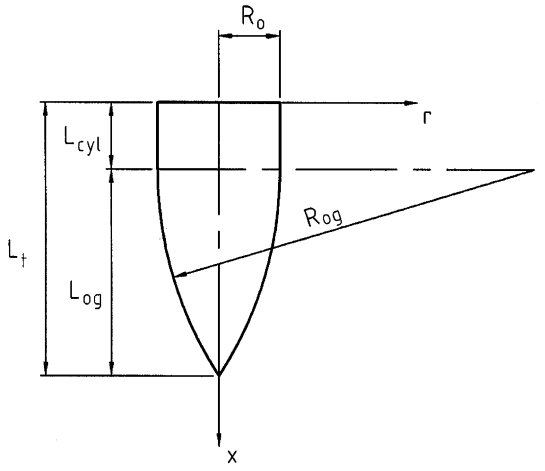

Fig. 3. Geometry of ogival projectile.

where r_x is the radius of ogival nose at x-position, and is obtained by following relations:

$$\begin{aligned} r_x &= \sqrt{R_{\mathrm{og}}^2 - (x - L_{\mathrm{cyl}})^2} - (R_{\mathrm{og}} - R_0); \quad L_{\mathrm{cyl}} < x < L_{\mathrm{t}} \\ r_x &= R_0; \quad x < L_{\mathrm{cyl}} \end{aligned} \tag{16}$$

where R_0 is the radius of projectile at cylindrical region, R_{og} is the curvature radius of ogival nose, L_{cyl} is the cylindrical length and L_{t} is the total length of projectile.

2.2. Rigid penetration analysis of a projectile into a semi-infinite target

During penetration of the projectile into the target, it is assumed that the nose geometry of projectile, which is in contact with cavity surface, is a part of a sphere. By progressing of penetration and further deformation of the projectile, the nose geometry can be converted to a hemisphere, and after more deformation and edge inversion, to hemisphere with cylindrical extension. In rigid penetration analysis of the projectile, a method has been used similar to Forrestal's model (1988, 1991) presented for rigid penetration analysis of a projectile with hemispherical nose.

By considering normal stress (σ_{n}) and tangential stress ($\sigma_{\mathrm{t}} = \mu\sigma_{\mathrm{n}}$) due to friction, and calculating the axial components and integrating on the nose surface, the axial force on the projectile, whose direction is opposite of the motion, is obtained by

$$F_z = \pi r_{\mathrm{n}}^2 \int_0^{\theta_{\mathrm{n}}} \sigma_{\mathrm{n}}(V,\theta)[\sin 2\theta + 2\mu \sin^2\theta]\,\mathrm{d}\theta \tag{17}$$

where r_{n} and θ_{n} have been shown in Fig. 4.

The velocity of the target particles in the interface of projectile and cavity, due to rigid penetration with velocity V, is

$$V_r(V,\theta) = V\cos\theta \tag{18}$$

Using results of spherical cavity expansion theory, the radial stress on the cavity surface or the normal stress on the nose of projectile is obtained by

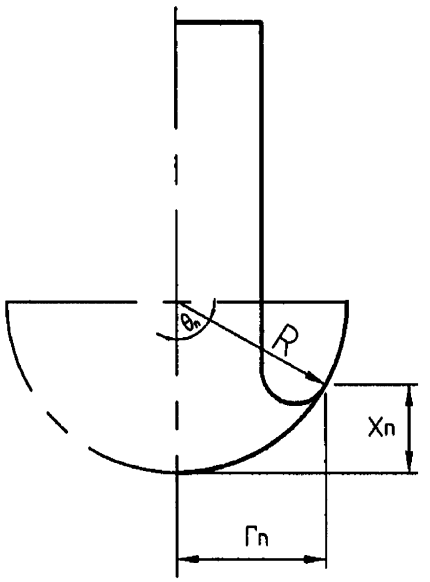

Fig. 4. Geometrical parameters of projectile nose.

$$\sigma_{\mathrm{n}}(V,\theta)/Y_{\mathrm{t}} = A_{\mathrm{s}} + B_{\mathrm{s}}\left[\left(\frac{\rho_{\mathrm{t}}}{Y_{\mathrm{t}}}\right)^{1/2} V\cos\theta\right]^2 \tag{19}$$

$$A_{\mathrm{s}} = \frac{2}{3}\left\{1 + \ln\left[\frac{E_{\mathrm{t}}}{3(1-\nu_{\mathrm{t}})Y_{\mathrm{t}}}\right]\right\}, \quad B_{\mathrm{s}} = 3/2 \tag{20}$$

where Y_{t}, ρ_{t}, E_{t} and ν_{t} are yield strength, density, Young's modulus and Poisson's ratio of the target, respectively, and the constants A_{s} and B_{s} are given for incompressible elastic-perfectly plastic target.

Substituting σ_{n} from (19) to (17), resistant axial force F_z on the nose of the projectile is obtained by

$$F_z = \alpha_{\mathrm{n}} + \beta_{\mathrm{n}} V^2 \tag{21}$$

$$\begin{aligned}\alpha_{\mathrm{n}} &= \pi r_{\mathrm{n}}^2 Y_{\mathrm{t}} A_{\mathrm{s}}\left[\frac{1-\cos 2\theta_{\mathrm{n}}}{2} + \mu\left(\theta_{\mathrm{n}} - \frac{1}{2}\sin 2\theta_{\mathrm{n}}\right)\right]\\ \beta_{\mathrm{n}} &= \frac{1}{16}\pi r_{\mathrm{n}}^2 \rho_{\mathrm{t}} B_{\mathrm{s}}[5 - 4\cos 2\theta_{\mathrm{n}} - \cos 4\theta_{\mathrm{n}} + \mu(4\theta_{\mathrm{n}} - \sin 4\theta_{\mathrm{n}})]\end{aligned} \tag{22}$$

where angle θ_{n} is obtained from Fig. 4 as

$$\begin{aligned}\theta_{\mathrm{n}} &= tg^{-1}\left(\frac{r_1}{R - x_1}\right); \quad x_1 < R\\ \theta_{\mathrm{n}} &= \pi/2; \quad x_1 \geqslant R\end{aligned} \tag{23}$$

Also the projectile equation of motion is

$$m\left(\frac{\mathrm{d}V}{\mathrm{d}t}\right) = mV\left(\frac{\mathrm{d}V}{\mathrm{d}Z}\right) = -F_z \tag{24}$$

Thus, the increment of penetration depth is obtained by

$$\mathrm{d}Z = mV\,\mathrm{d}V/(-F_z) \tag{25}$$

For an independent problem of rigid projectile penetration analysis, the total depth of penetration is obtained by integrating Eq. (25) and using the axial force F_z from Eq. (21):

$$Z_f = \int_0^{Z_f} dZ = -\int_{Vo}^{0} (mV/F_Z)\,dV \tag{26}$$

2.3. Combination of the projectile deformation and rigid penetration analysis in a new method

In the method of incremental deformation and penetration analysis, in a step of projectile deformation, for a time increment dt, values of ds, dx, dy, dV and A are evaluated by solving Eqs. (1)–(5) and using relations (6)–(9), and the target is assumed rigid. Modified values of these variables are calculated by relations (10)–(14).

Then, in a step of rigid penetration, values of dV and dZ are obtained by relations (21)–(25), and modified values are calculated by following relations:

$$V^{m+1} = V^m - dV \tag{27}$$

$$Z^{m+1} = Z^m + dZ \tag{28}$$

Initial conditions in this process are defined as

$$s = 0, \quad x = L_0, \quad y = 0, \quad V = V_0, \quad A = A_0, \quad Z = 0$$

where L_0, V_0 and A_0 are initial length, striking velocity and initial cross-section of projectile.

Incremental calculations of the problem are performed in successive steps of deformation and rigid penetration. These steps are continued until the projectile is stopped. Consequently, the total depth of penetration (Z_f) of the projectile is obtained by summing the increments dZ.

3. Terminal ballistic tests

For comparison of results, a series of ballistic tests have been carried out by using cylindrical projectiles with ogival nose, 6.7 mm diameter, 34.4 mm length and 7.7 g mass and 30×30 cm target plates with 25 mm thickness. The schematic setup of experiments, is shown in Fig. 5.

Four kinds of steel with different strength and hardness have been used in the tests for projectiles and targets. Also, the striking velocity of projectile has been programmed at three levels: 650, 750 and 850 m/s.

At least four repetitions have been done for each type of test and totally 210 ballistic tests were carried out, which some results have been presented in this paper for comparison.

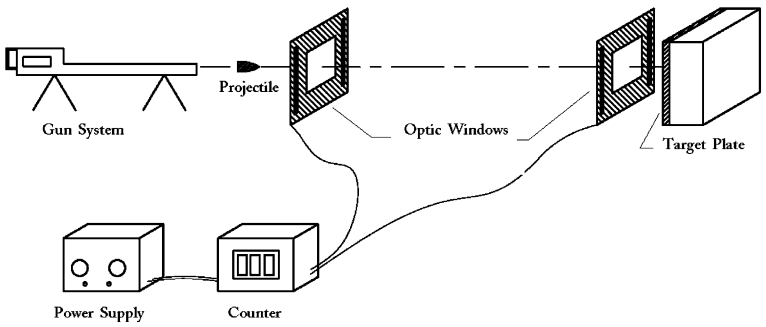

Fig. 5. Terminal ballistic tests setup.

The initial velocity of projectiles have been measured by two optic windows. An oscillator device starts to count when a projectile passes through the first window. Then the counter is stopped, when it passes through the second window. The passing time of the projectile between the windows is measured, and then the average velocity is calculated by dividing the distance by the time.

4. Numerical simulation

Simulation of the process has been done using the LS-DYNA code. The projectile and the target have been modeled by axisymmetric elements. Thus, the target plate has been considered as a cylinder with 60 mm diameter (Fig. 6a).

Nodes of circumference of target cylinder have been fixed, and symmetry conditions have been used for nodes on symmetry axis.

The Johnson–Cook material model and Gruneisen equation of state have been used for both parts. In the initial simulation due to ogival nose of projectile and high deformation of elements at contact region, the running stopped after 18 μs and error message is received (Fig. 6b). Therefore the element failure ability of the Johnson–Cook model has been used for solving this problem. Thus, before the high deformation and receiving error message, critical elements are failed and deleted. By deletion of a few obtrusive elements, running is continued until the projectile stops. Numerical values of depth of penetration (DOP) have been measured from vertical distance of bottom of the cavity to the initial surface of the target plate.

5. Results and discussion

Two limit combinations of projectile and target(including hard projectile-soft target and soft projectile-relatively hard target) among sixteen combinations, have been selected for discussion in this paper.

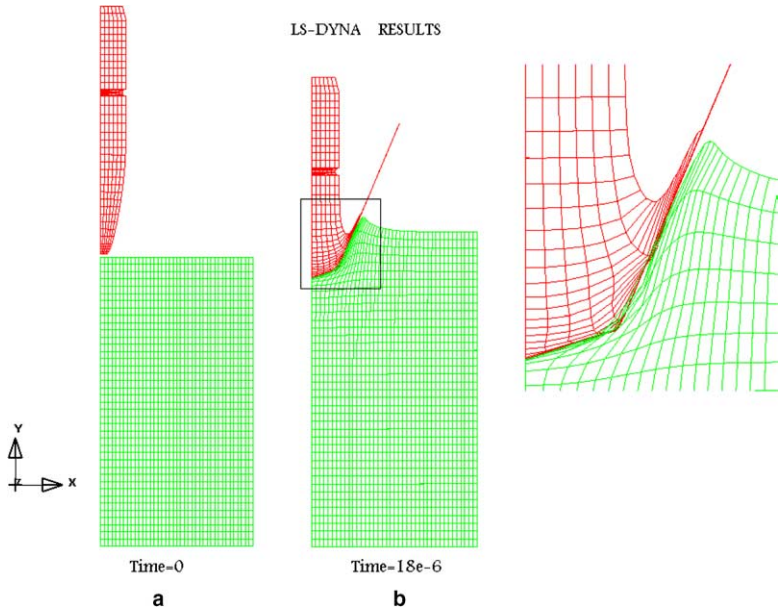

Fig. 6. (a) Finite element modeling of projectile and target, (b) deformation of elements at contact surface.

The yield strength (0.2% offset) and ultimate strength of projectiles and target plates have been given in Table 1, and analytical values of depth of penetration obtained from the new method, with experimental and numerical values from tests and simulations in Table 2.

Analytical, numerical and experimental results of test no. 19 (projectile M1, target P7 and striking velocity 760 m/s) have been given in Fig. 7 and shows qualitatively good agreement.

The graphs of penetration depth versus striking velocity for two combinations of projectile and target have been shown in Figs. 8 and 9. In these figures, it is obvious that with velocity in the range of 600–900 m/s, the values of penetration depth of projectile obtained from the analytical model have a very good agreement with respect to the experimental values at moderate to upper velocities. At lower velocities, results of the analytical model for depth of penetration are slightly higher than experimental values.

Also results of numerical simulations using LS-DYNA are in agreement with experimental values, in the range of applied velocity.

In addition the results of Forrestal's model for rigid penetration of a projectile with similar material and geometry including diameter and length, but with a spherical nose, have been shown in Figs. 8 and 9. These curves show that, the results of Forrestal's model for penetration depth are very high with respect to experimental and numerical values, in the applied conditions of materials and velocities. This fact is based on two

Table 1
Strengths of projectiles and target plates

Projectile			Target		
Code	Sy (MPa)	Su (MPa)	Code	Sy (MPa)	Su (MPa)
M3	308	496	P2	382	543
M1	533	603	P7	308	462

Table 2
Analytical, experimental and numerical values of penetration depth

Case	Test no.	V_0 (m/s)	Analytical DOP (mm)	Experimental DOP (mm)	Numerical DOP (mm)
Projectile: M3 Target: P2	120	858	8.2	8.50	8.86
	121	849	8.1	7.46	8.37
	122	851	8.1	7.51	8.58
	115	758	7.1	6.89	6.45
	116	750	7.0	6.15	6.23
	117	746	6.9	5.43	6.20
	111	650	5.8	4.32	3.98
	113	656	5.8	4.08	4.17
	114	630	5.5	4.61	3.66
Projectile: M1 Target: P7	14	858	9.4	10.65	9.36
	15	850	9.3	9.62	9.17
	16	846	9.2	9.15	9.03
	17	768	8.2	8.84	7.09
	19	760	8.1	6.46	7.06
	20	780	8.4	9.38	7.31
	21	648	6.6	2.99	4.57
	23	650	6.6	3.45	4.61
	24	660	6.7	4.97	4.76

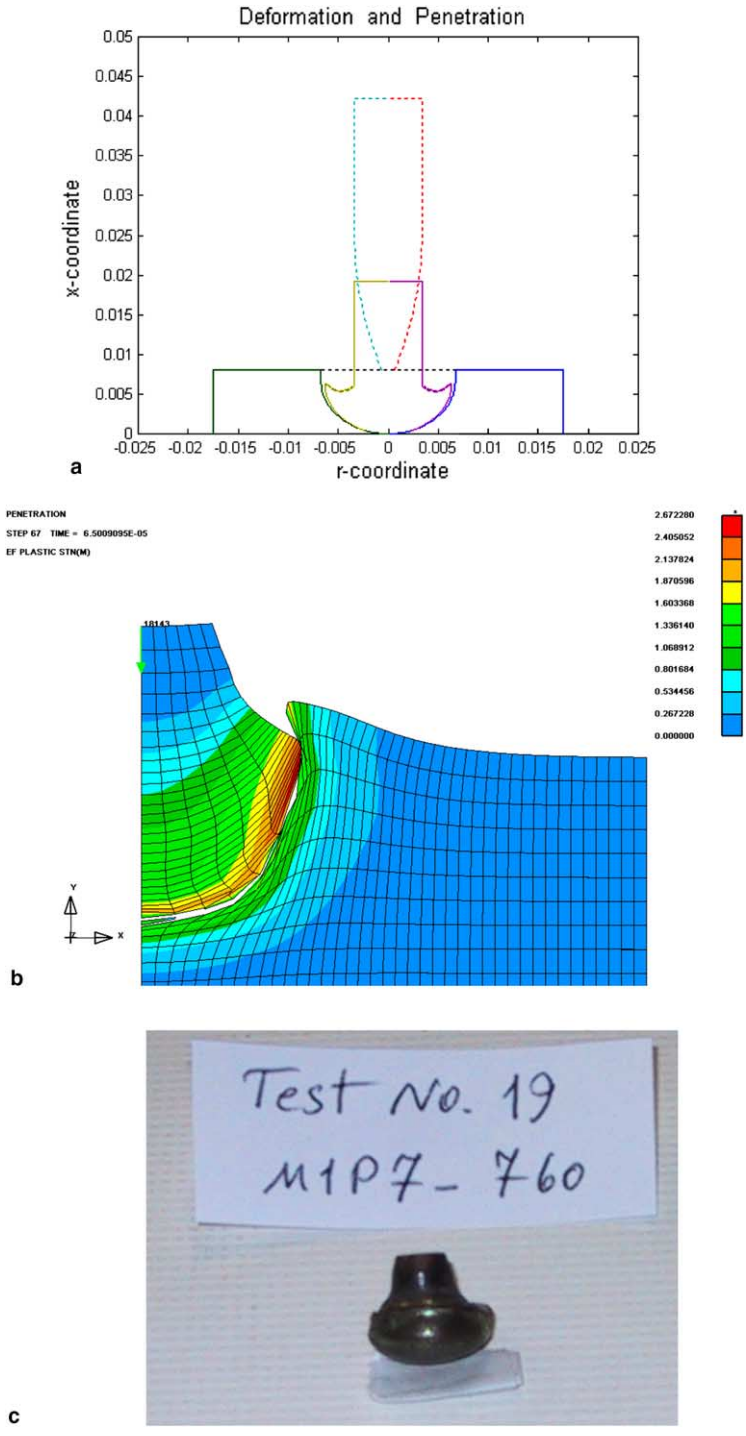

Fig. 7. Penetration analysis results (Projectile M1, Target P7, velocity = 760 m/s): (a) deformation and penetration from analytical modeling, (b) numerical simulation by LS-DYNA, (c) deformed projectile after ballistic test.

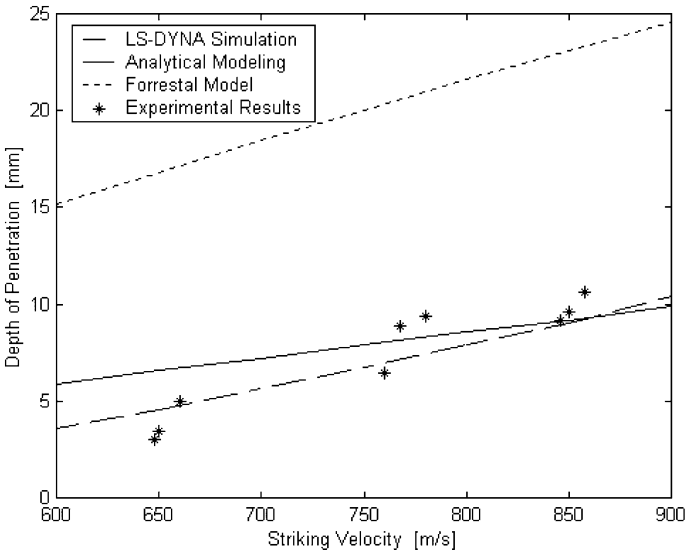

Fig. 8. The depth of penetration versus striking velocity (Projectile M1, Target P7).

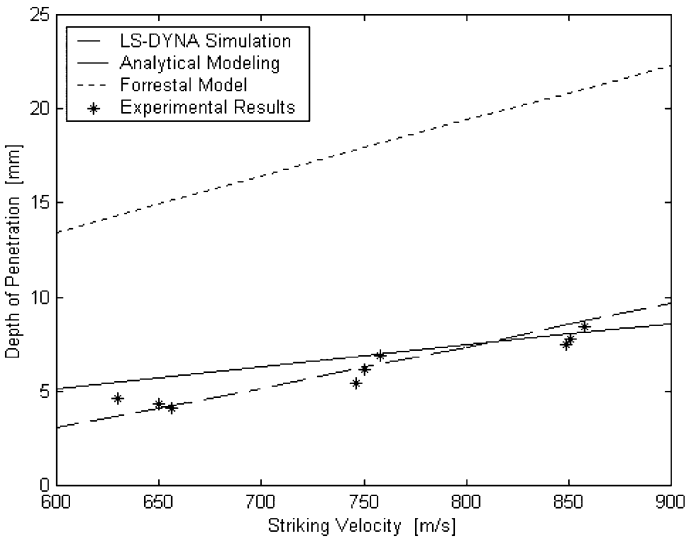

Fig. 9. The depth of penetration versus striking velocity (Projectile M3, Target P2).

main reasons in Forrestal's model. The first reason is the rigidity of the projectile without any mushrooming at nose, leads to more penetration. The second one is that there is no dissipation of kinetic energy due to projectile deformation. However in the analytical model presented in this paper, the mushrooming and dissipation of energy due to the projectile deformation have been considered, therefore it has given the better results in this conditions.

The difference of the analytical values, obtained by this model, with experimental results at lower velocities may be explained by two reasons. The first one related to the fact that the Forrestal's rigid penetration

model gives better results for deep penetration at higher velocities (Chen and Li, 2002), therefore this matter affects on rigid penetration steps of the new modeling. The second reason related to the assumption of constant cavity diameter, which has been considered in deformation steps of process. This assumption is almost correct at most of process at high striking velocities, but at lower striking velocities, it is valid only at the second half of process.

Totally this method has some advantages and disadvantages as follows:

Advantages:

1. This method presents a new idea for analysis of contact/penetration of projectile and target plate. In this method, the interaction between the projectile and target has been divided to two distinct parts, including rigid projectile-deformable target and deformable projectile-rigid target. Therefore, by some corrections in this method, an extensive range of problems, from perfectly rigid penetration into target plate to projectile mushrooming due to impact to rigid target, may be covered.
2. Although in this paper, the Hawkyard' model has been used for projectile deformation and Forrestal's model for rigid penetration, but other modified models may be used and replaced, for modifications.

Disadvantages:

1. The assumptions related to spherical contact surface of projectile and target, and constant cavity diameter (equal to twice of projectile diameter), although are not far from realistic views, but they may not be accurate.
2. Due to some difficulties, the ballistic tests have been carried out at a limited range of velocity (600–900 m/s), and limited range of strength for projectile and target materials. Thus, for extension of this method to a wide range of velocities and strengths, many other tests might be programmed.

6. Conclusion

In this paper, using two previous analytical models for deformation analysis and penetration analysis of a projectile, a new penetration analysis method for deformable projectile has been developed. In this method, deformation and penetration of projectile have been analyzed in separated, successive and incremental time steps. In each deformation step, the target was assumed rigid and the increment of the projectile deformation has been evaluated, using the Hawkyard's fundamental relations with some modifications. Also in each penetration step, the projectile has been assumed rigid and the increment of penetration of rigid projectile calculated using the Forrestal's model, based on cavity expansion theory and by some changes. Comparison of the penetration depth obtained by the new method with experimental values from a series of ballistic tests and numerical simulations by LS-DYNA shows good agreement, especially at velocities higher than 750 m/s. Therefore, this method can be used for considering the projectile deformation during penetration analysis. In addition, it seams that this method, by some considerations, may be used in an extensive range of problems, from perfectly rigid penetration into target plate to projectile mushrooming due to impact to rigid target.

References

Alekseevskii, V.P., 1966. Penetration of a rod into a target at high velocity. Combust. Explosion Shock Waves 2, 63–66.

Chen, X.W., Li, Q.M., 2002. Deep penetration of a non-deformable projectile with different geometrical characteristics. Int. J. Impact Eng. 27, 619–637.

Chen, X.W., Li, Q.M., 2004. Transition from nondeformable projectile penetration to semi-hydrodynamic penetration. ASCE J. Mech. Eng. 130 (1), 123–127.

Dikshit, S.N., Sundararajan, G., 1992. The penetration of thick steel plates by ogival shaped projectiles: experiments and analysis. Int. J. Impact Eng. 12, 373–408.

Forrestal, M.J., Okajima, K., Luk, V.K., 1988. Penetration of 6061-T651 Aluminum targets with rigid long rods. J. Appl. Mech. 55, 755–760.

Forrestal, M.J., Brar, N.S., Luk, V.K., 1991. Penetration of strain-hardening targets with rigid spherical-nose rods. J. Appl. Mech. 58, 7–10.

Hawkyard, J.B., 1969. Mushrooming of flat-ended projectiles impinging on a flat rigid anvil. IJMS 11, 313–319.

Jones, S.E., Gillis, P.P., 1987. On the penetration of semi-infinite targets by long rods. J. Mech. Phys. Solids 35, 121–131.

Khodarahmi, H., Fallahi, A., Liaghat, G.H., 2003. Penetration analysis of deformable projectile into metallic target. Ph.D. thesis, Amirkabir University of Technology, Tehran, Iran.

Liaghat, G.H., Malekzadeh, A., 1999. A modification to the mathematical model of penetration by Dikshit and Sundararajan. Int. J. Impact Eng. 22, 543–550.

LS-DYNA Theory Manual, 2001. Livermore Software Technology Corporation.

Luk, V.K., Piekutowski, A.J., 1991. An analytical model on penetration of eroding long rods into metallic targets. Ing. J. Impact Eng. 11, 323–340.

Ravid, M., Bodner, S.R., 1994. A two-dimensional analysis of penetration by an eroding projectile. Int. J. Impact Eng. 15, 587–603.

Recht, R.F., 1967. Ballistic Perforation Dynamics of Armor-Peircing Projectile. NWC TP4532, Naval Weapons Center, China Lake, CA.

Roisman, I.V., Yarin, A.L., Rubin, M.B., 1997. Oblique penetration of a rigid projectile into an elastic–plastic target. Int. J. Impact Eng. 19, 769–795.

Roisman, I.V., Yarin, A.L., Rubin, M.B., 2001. Normal penetration of an eroding projectile into an elastic–plastic target. Int. J. Impact Eng. 25, 573–597.

Rubin, M.B., Yarin, A.L., 2002. A generalized formula for the penetration depth of a deformable projectile. Int. J. Impact Eng. 27, 387–398.

Tate, A., 1967. A theory for the deceleration of long rods after impact. J. Mech. Phys. Solids 15, 387–399.

Woodward, R.L., 1982. Penetration of semi-infinite metal targets by deforming projectile. Int. J. Mech. Sci. 24, 73–87.

Yarin, A.L., Rubin, M.B., Roisman, I.V., 1995. Penetration of a rigid projectile into an elastic–plastic target of finite thickness. Int. J. Impact Eng. 16, 801–831.

Yaziv, D., Riegel, J.P., 1993. The application of the integral theory of impact to model penetration of hypervelocity impact. Int. J. Impact Eng. 14, 843–850.

Yossifon, G., Rubin, M.B., Yarin, A.L., 2001. Penetration of a rigid projectile into a finite thickness elastic–plastic target—comparison between theory and numerical computations. Int. J. Impact Eng. 25, 265–290.